Novel Rare Earth Polyborates. 2. Syntheses and Structures†

Linyan Li,‡ Xianglin Jin,§ Guobao Li,‡ Yingxia Wang,‡ Fuhui Liao,‡ Guangqin Yao,‡ and Jianhua Lin*,‡

State Key Laboratory of Rare Earth Materials Chemistry and Applications, College of Chemistry and Molecular Engineering, Peking University, Beijing 100871, People's Republic of China, and State Key Laboratory of Molecular Dynamic and Stable Structures, College of Chemistry and Molecular Engineering, Peking University, Beijing 100871, People's Republic of China

Received January 2, 2003. Revised Manuscript Received March 28, 2003

Three novel hydrated rare earth polyborates, $Ln[B_8O_{11}(OH)_5]$ (Ln = La−Nd) (**1**), $Ln[B_9O_{13}(OH)_4]\cdot H_2O$ (Ln = Pr − Eu) (**2**), and $Ce[B_5O_8(OH)]NO_3\cdot 3H_2O$ (**3**) have been synthesized by using boric acid as a flux at 240 °C, starting from rare earth oxides or nitrates and an excess of boric acid. All these polyborates crystallize in monoclinic structures ($P2_1/n$) and consist of borate sheets as the fundamental unit, that is, $[LnB_6O_{11}]$ sheet in **1** and **2** and $[CeB_5O_9]$ sheet in **3**. The borate sheets all contain a nine-membered borate ring, of which the rare earth cations are located around the center. The borate frameworks in **1** and **3** are two-dimensional, which are interlinked via ionic Ln−O bonds forming 3D structures. While in **2** the borate framework is three-dimensional with small channels filled by water molecules. Annealing the hydrated polyborates **1** and **2** at moderate temperature leads to two anhydrous pentaborates, α-LnB_5O_9 (**4**) for Ln = Pr−Eu and β-LnB_5O_9 (**5**) for Ln = La, Ce. The structure of β-LaB_5O_9 has been determined by an ab initio method using powder X-ray diffraction data. It crystallizes in a monoclinic structure in the space group $P2_1/c$ with a = 6.4418(1) Å, b = 11.6888(3) Å, c = 8.1706(2) Å, and β = 105.167(1)°. The structure of β-LnB_5O_9 contains buckled nine-membered ring borate sheets that are interlinked by BO_3 groups forming a three-dimensional framework. The Eu^{3+}-doped β-LaB_5O_9 materials show dominant $^5D_0 \rightarrow {}^7F_2$ emission and a low quenching concentration (0.6 at. %).

Introduction

Rare earth borates have long been the subject of interest as hosts of luminescent materials for their high transparency and exceptional optical damage threshold and high luminescence efficiency, particularly under VUV excitation. Most of such studies, however, focused on the three rare earth borates, that is, oxyborates,[1,2] orthoborates,[3,4] and metaborates.[5] They were actually the only three known rare earth borates thermodynamically stable in the Ln_2O_3−B_2O_3 (Ln = rare earth) system[6] at high temperature. According to the Lux-Flood acid−base concept, the small size and high local charge of the rare earth cation destabilize the polyborate framework;[7] the rare earth polyborates in the boron-rich region may not be stable at high temperature and thus remained largely unexploited. The other possible reason for this situation is the tendency to form glass phases for polyborates at high temperature. Recently, we proposed a low-temperature synthesis approach to hydrated rare earth polyborates by using boric acid as the flux,[8,9] and annealing the hydrated polyborates $Ln[B_6O_9(OH)_3]$ (Ln = Sm−Lu) at moderate temperature led to novel anhydrous rare earth polyborates α-LnB_5O_9 (Ln = Sm−Er). From a synthesis methodology point of view, this is a typical precursor approach, where the hydrated polyborate is used as a single-molecule precursor. As a continuous effort, we applied this approach to the early lanthanides and found interesting borate chemistry both in synthetic and structural aspects. A series of new hydrated rare earth polyborates, that is, hydrated pentaborates, octaborates, and nonaborates, with related layered structures were obtained under slightly different reaction conditions. Thermal decom-

† The first part of this study has been published in *Chem. Mater.* **2002**, *14*, 4963−4968.

* To whom correspondence should be addressed. E-mail: jhlin@chem.pku.edu.cn. Tel.: (8610)62751715. Fax: (8610)62751708.

‡ State Key Laboratory of Rare Earth Materials Chemistry and Applications.

§ State Key Laboratory of Molecular Dynamic and Stable Structures.

(1) Lin, J. H.; Su, M. Z.; Wurst, K.; Schweda, E. *J. Solid State Chem.* **1996**, *126*, 287.

(2) Lin, J. H.; Zhou, S.; Yang, L. Q.; Yao, G. Q.; Su, M. Z.; You, L. P. *J. Solid State Chem.* **199**7, *134*, 158.

(3) Ren, M.; Lin, J. H.; Dong, Y.; Yang, L. Q.; Su, M. Z.; You, L. P. *Chem. Mater.* **1999**, *11*, 1576.

(4) Yang, Z.; Ren, M.; Lin, J. H.; Su, M. Z.; Tao, Y.; Wang, W. *Chem. J. Chin. Univ. (Chinese)* **2000**, *21* (9), 1339.

(5) Abdullaev, G. K.; Mamedov, Kh. S.; Dzhafarov, G. G. *Sov. Phys. Crystallogr.* **1975**, *20*, 161.

(6) Levin, E. M.; Robbins, C. R.; Warring, J. L. *J. Am. Ceram. Soc.* **1961**, *44*, 87.

(7) Leonyuk, N. I. *J. Cryst. Growth* **1997**, *174*, 301.

(8) Lu, P. C.; Wang, Y. X.; Lin, J. H.; You, L. P. *Chem. Commun.* **2001**, 1178.

(9) Li, L. Y.; Lu, P. C.; Wang, Y. Y.; Jin, X. L.; Li, G. B.; Wang, Y. X.; You, L. P.; Lin, J. H. *Chem. Mater.* **2002**, *14*, 4963.

10.1021/cm030004d CCC: $25.00
Published on Web 04/25/2003

Table 1. Typical Synthesis Conditions of the Hydrated Polyborates (Ln = La−Eu)

reactant	starting molar ratio (B/Ln)	temp (°C)	product
La_2O_3, H_3BO_3	30:1	240	$La[B_8O_{11}(OH)_5]$
	15:1	240	$La[B_8O_{11}(OH)_5]$
CeO_2, H_3BO_3	30:1	240	$Ce[B_8O_{11}(OH)_5] + CeO_2$
	15:1	240	$Ce[B_8O_{11}(OH)_5] + CeO_2$
$Ce(NO_3)_3{\cdot}6H_2O$, H_3BO_3	30:1	240	$Ce[B_5O_8(OH)]NO_3{\cdot}3H_2O$ + $Ce[B_8O_{11}(OH)_5]$ (minor)
	15:1	240	$Ce[B_5O_8(OH)]NO_3{\cdot}3H_2O$ + $Ce[B_8O_{11}(OH)_5]$ (minor)
Pr_6O_{11}, H_3BO_3	30:1	240	$Pr[B_8O_{11}(OH)_5]$
	15:1	240	$Pr[B_9O_{13}(OH)_4]{\cdot}H_2O$
Nd_2O_3, H_3BO_3	30:1	240	$Nd[B_8O_{11}(OH)_5]$ (minor) + $Nd[B_9O_{13}(OH)_4]{\cdot}H_2O$
	15:1	240	$Nd[B_9O_{13}(OH)_4]{\cdot}H_2O$
Sm_2O_3, H_3BO_3	30:1	240	$Sm[B_6O_9(OH)_3]$[9]
	15:1	240	$Sm[B_9O_{13}(OH)_4]{\cdot}H_2O$
Eu_2O_3, H_3BO_3	30:1	240	$Eu[B_6O_9(OH)_3]$[9]
	15:1	240	$Eu[B_9O_{13}(OH)_4]{\cdot}H_2O$

position of these hydrated polyborates yielded two different types of anhydrous pentaborates, that is, the α- and β-polymorphs of LnB_5O_9. Here, in this report we describe the syntheses and structures of these polyborates, as well as a preliminary study on the luminescent property of the europium-doped β-LaB_5O_9.

Experimental Section

Synthesis of Hydrated Polyborates. The hydrated rare earth polyborates, that is, octaborates, nonaborates, and pentaborates, were synthesized in a flux of boric acid, H_3BO_3 (analytical grade), along with rare earth oxides, La_2O_3, CeO_2, Pr_6O_{11}, Nd_2O_3, Sm_2O_3, and Eu_2O_3 (all with purity of 99.99%) or $Ce(NO)_3{\cdot}6H_2O$ (99.99%). The general procedure of the syntheses is as follows: rare earth oxide or nitrate was mixed with H_3BO_3 in a B/Ln mole ratio varying from 15:1 to 30:1 and charged into Teflon autoclaves. The reactions were carried out at 240 °C for about 5 days. The excess of boric acid was removed by washing the products with hot distilled water, and the products were then dried at 80 °C for 10 h. Depending on the rare earths and the B/Ln ratios in the starting materials, three different types of new hydrated polyborates were obtained, that is, octaborate $Ln[B_8O_{11}(OH)_5]$ (**1**), nonaborate $Ln[B_9O_{13}(OH)_4]{\cdot}H_2O$ (**2**), and pentaborate $Ce[B_5O_8(OH)]NO_3{\cdot}3H_2O$ (**3**). Table 1 summarizes the typical synthesis conditions and the products.

Synthesis of Anhydrous Pentaborates. Two different types of anhydrous pentaborates, namely, α-LnB_5O_9 (**4**) and β-LnB_5O_9 (**5**), were synthesized by heating the hydrated rare earth polyborates **1** and **2** at moderate temperatures. Compounds **5** with a new polyborate structure type were obtained by heating **1** (Ln = La and Ce) at 850 °C for 2 days. Compounds **4**, which are isostructural to GdB_5O_9,[8,9] were obtained by heating **1** (Ln = Pr and Nd) and **2** at 700 °C for 2 days.

Powder X-ray diffraction patterns were recorded on a Rigaku D/max-2000 diffractometer with graphite monochromatized Cu Kα radiation. The powder diffraction data used for structure determination was collected on a Bruker D8-Advance diffractometer with Cu $K\alpha_1$ radiation. Chemical analysis was carried out by an ICP method. DTA and TGA measurements were carried out on a Dupont 1090 instrument under a N_2 atmosphere with a heating rate of 5 °C/min. IR spectra were recorded on a Nickel Magna-750 FT-IR spectrometer. Photoluminescence spectra were recorded with a F-4500 fluorescence spectrophotometer.

X-ray Crystallographic Studies. Crystal structures of the hydrated rare earth octaborates (**1**), nonaborates (**2**), and cerium pentaborate (**3**) were determined by single-crystal X-ray diffraction techniques, where crystals of $Pr[B_8O_{11}(OH)_5]$, $Nd[B_9O_{13}(OH)_4]{\cdot}H_2O$, and $Ce[B_5O_8(OH)]NO_3{\cdot}3H_2O$ with the dimensions 0.60 × 0.25 × 0.10, 0.20 × 0.15 × 0.05, and 0.25 × 0.20 × 0.08 mm^3, respectively, were used for data collections on a Rigaku R-AXIS RAPID image plate diffractometer with graphite monochromated Mo Kα radiation (λ = 0.71073 Å). Absorption corrections were applied based on symmetry-equivalent reflections using the ABSOR program.[10] All of the three hydrated polyborates crystallize in the monoclinic space group $P2_1/n$ with the lattice constants of a = 9.860(2) Å, b = 14.131(3) Å, c = 7.940(2) Å, and β = 89.79(3)° for $Pr[B_8O_{11}(OH)_5]$, a = 9.871(2) Å, b = 16.696(3) Å, c = 7.716(2) Å, and β = 90.12(3)° for $Nd[B_9O_{13}(OH)_4]{\cdot}H_2O$, and a = 6.465(1) Å, b = 15.571(3) Å, c = 10.656(2) Å, and β = 90.24(3)° for $Ce[B_5O_8(OH)]NO_3{\cdot}3H_2O$. The crystal structures were established by using direct methods (SHELXS97)[11] and subsequent different Fourier analyses. The final refinements were carried out by full-matrix least squares on F^2 using all unique data with SHELXL97[11] with the anisotropic displacement parameters for all non-hydrogen atoms. The crystallographic data and refined parameters are listed in Table 2. Selected bond lengths are listed in Table 3. The details of the structural parameters are included in the Supporting Information. The other lanthanides also form similar compounds; that is, $Ln[B_8O_{11}(OH)_5]$ (**1**) for Ln from La to Nd and $Ln[B_9O_{13}(OH)_4]H_2O$ (**2**) for Ln from Pr to Eu, are isostructural to these structures as confirmed by powder X-ray diffraction patterns. Table 4 lists the unit cell parameters obtained by indexing the powder diffraction data.

The α-LnB_5O_9 (Ln = Pr, Nd, Sm, and Eu) (**4**) compounds are isostructural with GdB_5O_9,[8,9] and their unit cell parameters are given in Table 4, while the β-LnB_5O_9 (Ln = La and Ce) (**5**) compounds crystallize in a new structure type. Because the β-LnB_5O_9 was obtained by decomposition of the hydrated polyborates, the product was always in polycrystalline form; thus, the structure was determined by the ab initio method using powder X-ray diffraction data. LaB_5O_9 crystallizes in the monoclinic space group $P2_1/c$ with the lattice constants of a = 6.4418(1) Å, b = 11.6888(3) Å, c = 8.1706(2) Å, and β = 105.167(1)°. Optimal estimates of the individual reflection intensities were extracted by a profile-fitting method using EXTRA.[12] The direct method with Sirpow-92[13] was able to locate all atoms in the structure including one lanthanum, nine oxygens, and five borons. The structure was then refined with

Table 2. Crystallographic Data for $Pr[B_8O_{11}(OH)_5]$, $Nd[B_9O_{13}(OH)_4]{\cdot}H_2O$, $Ce[B_5O_8(OH)]NO_3{\cdot}3H_2O$, and LaB_5O_9

formula	$Pr[B_8O_{11}(OH)_5]$	$Nd[B_9O_{13}(OH)_4]{\cdot}H_2O$	$Ce[B_5O_8(OH)]NO_3{\cdot}3H_2O$	LaB_5O_9
formula mass	488.42	535.57	455.22	336.95
space group	$P2_1/n$	$P2_1/n$	$P2_1/n$	$P2_1/c$
a (Å)	9.860(2)	9.871(2)	6.465(1)	6.4418(1)
b (Å)	14.131(3)	16.696(3)	15.571(3)	11.6888(3)
c (Å)	7.940(2)	7.716(2)	10.656(2)	8.1706(2)
β (deg)	89.79(3)	90.12(3)	90.24(3)	105.167(1)
V (Å^3)	1106.3(4)	1271.6(5)	1072.7(3)	593.8(1)
Z	4	4	4	4
T (K)	293	293	293	293
λ (Å)	0.71073	0.71073	0.71073	1.5405
ρ_{calcd} (g/cm^3)	2.934	2.799	2.820	3.77
μ(Mo Kα) (mm^{-1})	4.511	4.131	4.205	
diffraction technique	single-crystal X-ray diffraction			powder X-ray diffraction
R indices ($I > 2\sigma$)	R1 = 0.0412, wR2 = 0.1099	R1 = 0.0235, wR2 = 0.0563	R1 = 0.0557, wR2 = 0.1282	Rp = 0.0699, Rwp = 0.1072

Table 3. Selected Bond Distances (Å) for $Pr[B_8O_{11}(OH)_5]$, $Nd[B_9O_{13}(OH)_4]\cdot H_2O$, and $Ce[B_5O_8(OH)]NO_3\cdot 3H_2O$

$Pr[B_8O_{11}(OH)_5]$				$Nd[B_9O_{13}(OH)_4]\cdot H_2O$		$Ce[B_5O_8(OH)]NO_3\cdot 3H_2O$	
bond	distance	bond	distance	bond	distance	bond	distance
Pr(1A)−O(1)	2.569(4)	Pr(1B)−O(1)	2.600(7)	Nd(1)−O(2)	2.575(2)	Ce(1)−O(1)	2.646(6)
Pr(1A)−O(2)	2.578(4)	Pr(1B)−O(2)	2.484(7)	Nd(1)−O(4)	2.610(2)	Ce(1)−O(2)	2.642(6)
Pr(1A)−O(4)	2.636(4)	Pr(1B)−O(4)	2.403(9)	Nd(1)−O(5)	2.503(2)	Ce(1)−O(3)	2.620(7)
Pr(1A)−O(5)	2.551(4)	Pr(1B)−O(5)	2.673(8)	Nd(1)−O(6)	2.485(2)	Ce(1)−O(4)	2.583(6)
Pr(1A)−O(7)	2.739(4)	Pr(1B)−O(7)	2.395(11)	Nd(1)−O(7)	2.511(2)	Ce(1)−O(6)	2.548(6)
Pr(1A)−O(10)	2.585(4)	Pr(1B)−O(10)	2.638(8)	Nd(1)−O(8)	2.530(2)	Ce(1)−O(8)	2.639(7)
Pr(1A)−O(11)	2.470(5)	Pr(1B)−O(11)	2.942(16)	Nd(1)−O(12)	2.433(2)	Ce(1)−O(9)	2.558(7)
Pr(1A)−O(12)	2.359(4)	Pr(1B)−O(12)	2.620(12)	Nd(1)−O(13)	2.354(2)	Ce(1)−O(10)	2.540(8)
Pr(1A)−O(14)	2.724(5)	Pr(1B)−O(14)	2.249(16)	Nd(1)−O(16)	2.475(2)	Ce(1)−O(11)	2.571(8)
Pr(1A)−O(16)	2.753(6)					Ce(1)−O(12)	2.515(8)

Table 4. Unit Cell Parameters of the Rare Earth Polyborates

compound	space group	*a* (Å)	*b* (Å)	*c* (Å)	*β* (deg)
$Ce[B_5O_8(OH)]NO_3$	$P2_1/n$	6.465(1)	15.571(3)	10.656(2)	90.24(3)
$La[B_8O_{11}(OH)_5]$	$P2_1/n$	9.8994(3)	14.2678(3)	7.9934(2)	90.061(4)
$Ce[B_8O_{11}(OH)_5]$	$P2_1/n$	9.8726(9)	14.1875(4)	7.9610(8)	90.064(15)
$Pr[B_8O_{11}(OH)_5]$	$P2_1/n$	9.8461(9)	14.1621(4)	7.9270(8)	90.065(17)
$Nd[B_8O_{11}(OH)_5]$	$P2_1/n$	9.8256(20)	14.2054(6)	7.9140(17)	90.140(37)
$Pr[B_9O_{13}(OH)_4]$	$P2_1/n$	9.8947(17)	16.7533(4)	7.7336(12)	90.035(33)
$Nd[B_9O_{13}(OH)_4]$	$P2_1/n$	9.8806(11)	16.6995(5)	7.7190(8)	90.087(2)
$Sm[B_9O_{13}(OH)_4]$	$P2_1/n$	9.8538(9)	16.5877(4)	7.6887(7)	90.08(16)
$Eu[B_9O_{13}(OH)_4]$	$P2_1/n$	9.8589(8)	16.5673(5)	7.6917(6)	90.065(1)
β-LaB_5O_9	$P2_1/c$	6.4418(1)	11.6888(3)	8.1706(2)	105.167(1)
α-PrB_5O_9	I_1/acd	8.3912(2)		34.0541(16)	
α-NdB_5O_9	I_1/acd	8.3120(1)		33.7962(12)	
α-SmB_5O_9	I_1/acd	8.2789(4)		33.7320(16)	
α-EuB_5O_9	I_1/acd	8.2556(2)		33.6625(13)	

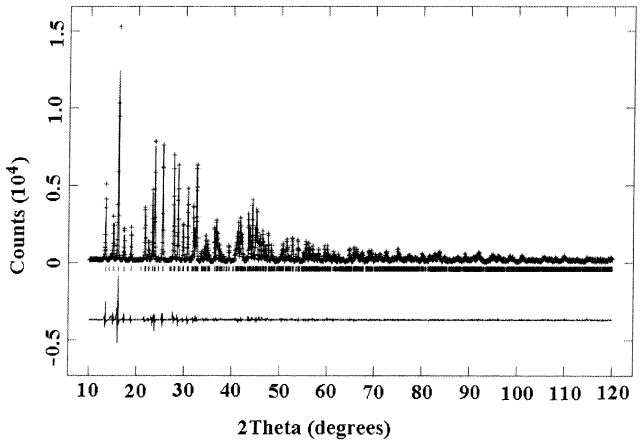

Figure 1. Profile fit to the powder X-ray diffraction pattern of LaB_5O_9. The symbol + represents the observed value, solid line represents the calculated value; the marks below the diffraction patterns are the calculated reflection positions, and the difference curve is shown at the bottom of the figure.

the Rietveld method (GSAS[14]). The final refinement, with isotropic displacement parameters, yielded $R_p = 0.0699$ and $R_{wp} = 0.1072$. Figure 1 shows the profile fit of the diffraction pattern and the crystallographic data are given in Table 2. The detailed information about the structure parameters is included in the Supporting Information.

(10) Higashi, T. *ABSCOR, Empirical Absorption based on Fourier Series Approximation*; Rigaku Corporation: Tokyo, 1995.

(11) Sheldrick, G. M. *SHELXS 97, Program for the solution of crystal structures*; University of Göttingen: Göttingen, Germany, 1997. *SHELXL 97, Program for the refinement of crystal structures*; University of Göttingen: Göttingen, 1997.

(12) Altomare, A.; Burla, M. C.; Cascarano, G.; Giacovazzo, C.; Guagliardi, A.; Moliterni, A. G. G.; Polidori, G. *J. Appl. Crystallogr.* **1995**, *28*, 842.

(13) Altomare, A.; Cascarana, G.; Giacovazzo, C.; Guagliardi, A. *SIRPOW user's manual*; Inst. Di Ric. Per lo Sviluppo di Metodologie Cristallografiche, CNR.

(14) Larson, A. C.; von Dreele, R. B. Report LAUR 86-748; Los Alamos National Laboratory: Los Alamos, NM, 1985.

Results and Discussions

Synthesis Reactions. The synthesis of hydrated rare earth polyborates in the flux of boric acid is a simple acid−base reaction as shown in the following:

$$16H_3BO_3 + Ln_2O_3 \xrightarrow{240\ ^\circ C} 2Ln[B_8O_{11}(OH)_5] + 19H_2O \quad (Ln = La-Nd) \quad (1)$$

$$18H_3BO_3 + Ln_2O_3 \xrightarrow{240\ ^\circ C} 2Ln[B_9O_{13}(OH)_4]\cdot H_2O + 21H_2O \quad (Ln = Pr-Eu) \quad (2)$$

$$10H_3BO_3 + 2Ce(NO_3)_3 \xrightarrow{240\ ^\circ C} 2Ce[B_5O_8(OH)]NO_3\cdot 3H_2O + 4NO_2 + O_2 + 8H_2O \quad (3)$$

It can be seen from Table 1 that the products depend crucially on the lanthanides and the ratio of B/Ln in the starting materials. The larger cations tend to form hydrated octaborates **1**, and smaller cations prefer hydrated nonaborates **2**. The hydrated pentaborate **3** was found only for cerium starting from cerium nitrate. The reaction of boric acid and CeO_2 was slow and, in addition to $Ce[B_8O_{11}(OH)_5]$, the products always contain a considerable amount of CeO_2. The ratio of B/Ln in the starting materials also shows substantial influence on the products. In general, the octaborates **1** tend to be formed for high B/Ln ratio, while the nonaborates **2** are preferred for low B/Ln. This finding was used extensively to synthesize the single-phase products. For example, the single-phase product of **2** can be obtained for Ln = Pr, Nd, Sm, and Eu with B/Ln ≤ 15, whereas similar reactions but with high B/Ln ≈ 30 yielded single-phase product of **1** for La and Pr, a mixture of **1** and **2**

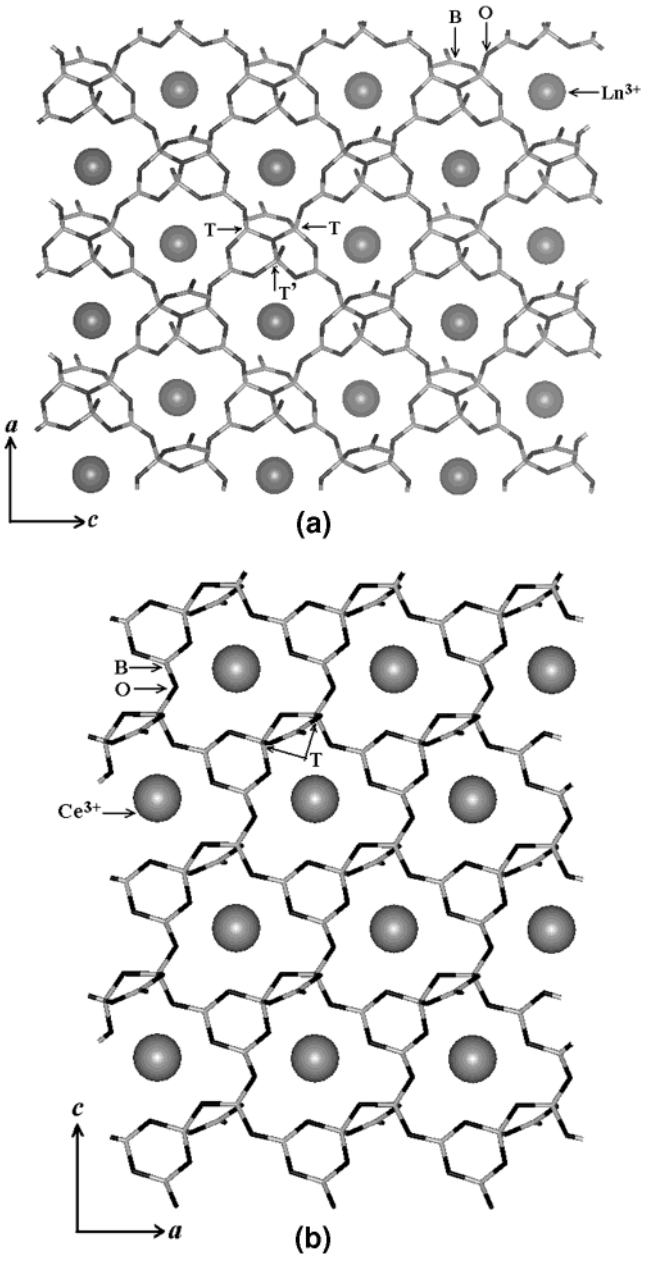

Figure 2. (a) $[LnB_6O_{11}]$ layer in $Ln[B_8O_{11}(OH)_5]$ and $Ln[B_9O_{13}(OH)_4]\cdot H_2O$; (b) $[LnB_5O_9]$ layer in $Ce[B_5O_8(OH)]NO_3\cdot 3H_2O$. The borate network is displayed in stick style, and the balls represent the rare earth cations.

for Nd, and a single phase of hexaborates $Ln[B_6O_9(OH)_3]$ for Sm and Eu.[9] We also found that water in the starting materials may influence the products. A general trend is that the additional water added to the system favors more hydrated products. For example, a small amount of water (about 1 mL in this study) added to the starting materials leads to the formation of $Ln[B_8O_{11}(OH)_5]$ and $Ln[B_6O_9(OH)_3]$, even if the B/Ln = 15.

Anhydrous pentaborates were synthesized via decomposition of the hydrated polyborates. Two types of pentaborates were obtained by heating **1** and **2** at about 700−850 °C. In fact, the products depend only on the lanthanides no matter what hydrated polyborates are used. Compounds **4** were obtained for smaller rare earth cations from Pr^{3+} to Eu^{3+}. Compounds **5** can only be observed for the large rare earth cations for La^{3+}

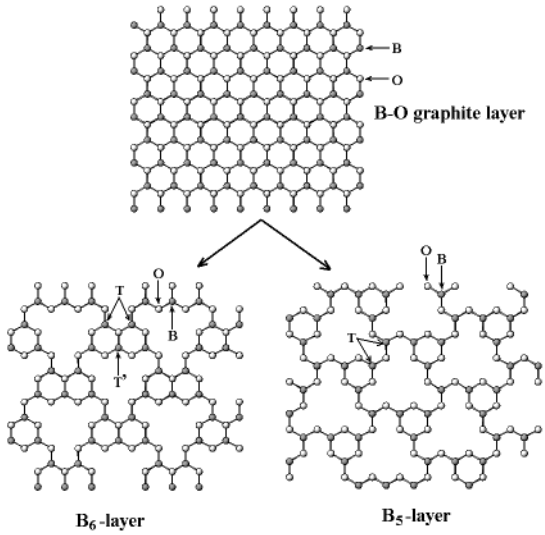

Figure 3. Hypothetical graphite-like [BO] sheet and its two variants, i.e., B_6-layer and B_5-layer. The B_6-layer and B_5-layer are formed by removal of one B_3O unit in every 8[BO] unit and every 7[BO] unit, respectively. The dark balls represent boron atoms, and the gray balls represent oxygen atoms.

and Ce^{3+}. The decomposition reaction of the hydrated polyborates can be expressed as follows.

$$2Ln[B_8O_{11}(OH)_5] \rightarrow 2\beta\text{-}LnB_5O_9 + 3B_2O_3 + 5H_2O \quad (Ln = La, Ce) \quad (4)$$

$$2Ln[B_8O_{11}(OH)_5] \rightarrow 2\alpha\text{-}LnB_5O_9 + 3B_2O_3 + 5H_2O \quad (Ln = Pr, Nd) \quad (5)$$

$$2Ln[B_9O_{13}(OH)_4] \rightarrow 2\alpha\text{-}LnB_5O_9 + 2B_2O_3 + 3H_2O \quad (Ln = Pr-Eu) \quad (6)$$

B_2O_3 in the products was not observable in the XRD patterns, which, as expected, may exist in amorphous form. Decomposition of $Ce[B_5O_8(OH)]NO_3\cdot 3H_2O$ (**3**) at 850 °C in air also forms β-CeB_5O_9, but contains CeO_2 as a second phase.

Crystal Structures of Hydrated Rare Earth Polyborates. All of these hydrated rare earth polyborates can be described as borate layers that stack one over another, forming the polyborate structures. Two different borate layers were identified in **1**, **2**, and **3**. The one in **1** and **2** is the $[LnB_6O_{11}]$ layer as shown in Figure 2a and the other in **3** is the $[LnB_5O_9]$ layer as shown in Figure 2b. A common feature of these borate layers is that they all contain nine-membered ring windows with rare earth cations locating at the center. These borate layers could be derived from a hypothetical graphite net (BO) (Figure 3) by removing the B_3O unit. The nine-membered-ring sheet in the $[LnB_6O_{11}]$ layer is obtained by removing B_3O in every 8BO unit in an ordered way (named B_6-layer in Figure 3), while removing B_3O in every 7BO unit results in the nine-membered-ring sheet in the $[LnB_5O_9]$ layer (named B_5-layer in Figure 3). In comparison to the hypothetical nine-membered-ring sheets with those in the real structures (Figure 2), one can easily find their similarity and relationship. One should pay particular attention to the boron atoms labeled as T-sites and T′-site in the hypothetical B_6- and B_5-layers. Linking an additional BO_3 group and an additional oxygen atom to the T-sites

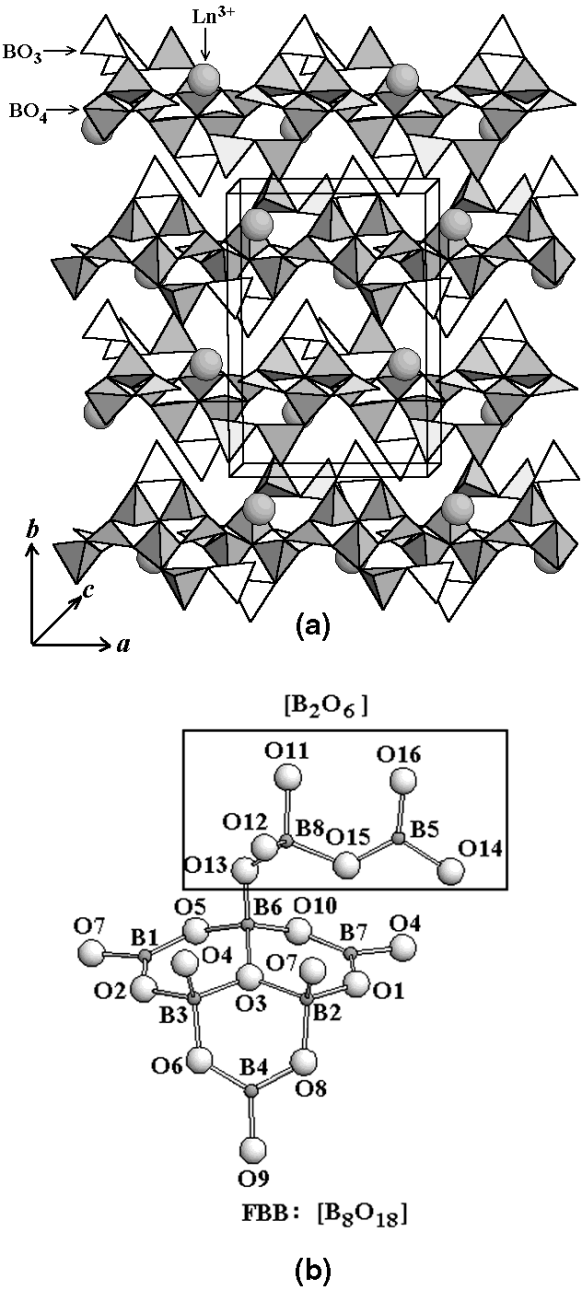

Figure 4. (a) An overview of the structure of $Ln[B_8O_{11}(OH)_5]$ and (b) the fundamental building block of $Ln[B_8O_{11}(OH)_5]$.

and the T′-site, respectively, in the B_6-layer will produce the $[LnB_6O_{11}]$ layer. Similarly, the $[LnB_5O_9]$ layer can be obtained by adding a BO_3 group to the T-sites in the B_5-layer. Since the borate layers contain BO_4 groups, both $[LnB_6O_{11}]$ and $[LnB_5O_9]$ layers are not planer but buckled. Starting from these fundamental borate layers, one could construct various polyborates either with known structures or with the new structure types in this study. For example, the Tunellite $(Sr[B_6O_9(OH)_2]\cdot 3H_2O)$ [15] structure can be obtained by simply stacking the $[LnB_6O_{11}]$ layers.

The terminal oxygen atom on the T′-site shown in Figure 2a in the $[LnB_6O_{11}]$ layer is of particular importance because this is an active position that could connect to an additional side-borate-chain to form more

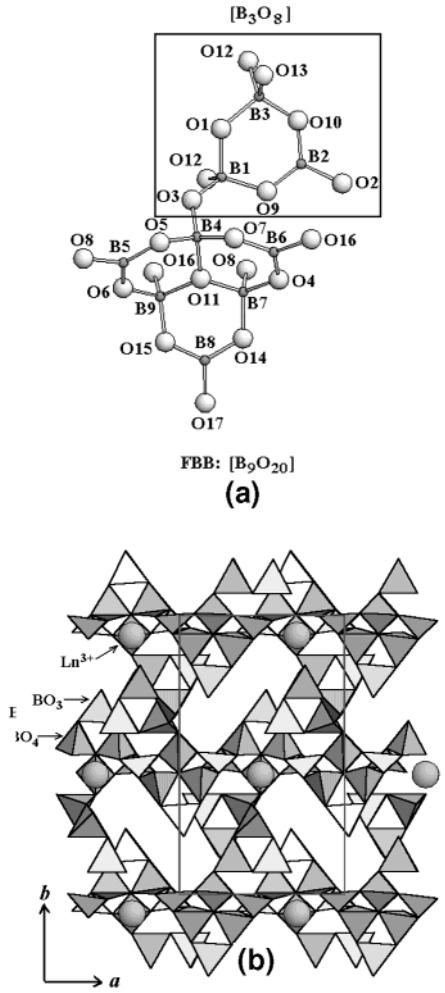

Figure 5. (a) Fundamental building block of $Ln[B_9O_{13}(OH)_4]\cdot H_2O$ and (b) structure of $Ln[B_9O_{13}(OH)_4]\cdot H_2O$ viewed along the (001) direction. The guest water molecules are omitted for clarity.

boron-rich compounds. In the structure of **1**, the side-borate-chain is the diborate $[B_2O_6]$ group sharing an oxygen atom on the T′-site in the $[LnB_6O_{11}]$ sheet, forming a two-dimensional borate layer, which is then stacked along the *b*-axis to form the structure (Figure 4a). The borate framework of **1** can also be described using a fundamental building block (FBB) consisting of $[B_6O_{13}]$ (noted as $3\Delta + 3T$) and $[B_2O_6]$ (as $1T + 1\Delta$)[16,17] as shown in Figure 4b. The $[B_6O_{13}]$ unit is a three-joint three-membered ring containing an unusual O atom bonded to three boron atoms. A similar borate unit was known in several known borates, such as tunellite and strontioborite.[18] The borate framework in **1** is two-dimensional, but the borate layers are interlinked by ionic Ln−O bonds so the structure is three-dimensional. Similarly, the FBB of **2** consists of a $[B_6O_{13}]$ unit ($3\Delta + 3T$) and a three-membered ring $[B_3O_8]$ ($1\Delta + 2T$) shown in Figure 5a. Unlike **1**, the side chains ($[B_3O_8]$ groups) from adjacent borate layers are condensed to a four-membered-ring unit $[B_6O_{14}]$ in **2**, resulting in a 3D porous borate framework as shown in Figure 5b. The

(15) Clark, J. R. *Am. Mineral.* **1964**, *49*, 1549.

(16) Christ, C. L.; Clark, J. R. *Phys. Chem. Miner.* **1977**, *2*, 59.
(17) Heller, G. *Topics in Current Chemistry 131*; Springer-Verlag: Berlin, 1986.
(18) Brovkin, A. A.; Zayakina, N. V.; Brovkina, V. S. *Sov. Phys.-Cryst.* **1975/1976**, *20*, 563; *Kristallografiya* **1975**, *20*, 911.

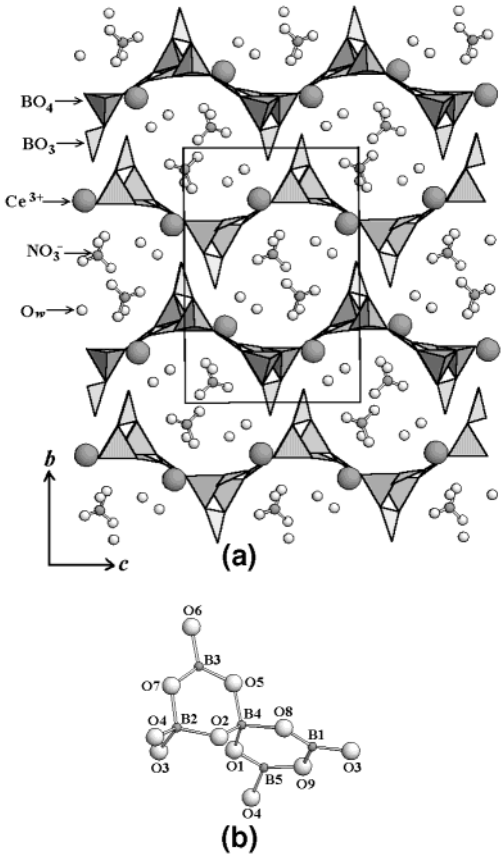

Figure 6. (a) An overview of structure of $Ce[B_5O_8(OH)]NO_3 \cdot 3H_2O$ projected along the *a*-axis. O_w represents the oxygen atoms of the guest water molecules. (b) Fundamental building block in the structure of $Ce[B_5O_8(OH)]NO_3 \cdot 3H_2O$.

cavities in the structure, however, are filled with water molecules. From the structure point of view, **1** and **2**, although they have different compositions, can be attributed to the same family of tunellite and strontioborite since all of them have a related borate layer of $6\infty_2$:($3\Delta + 3T$).

The structure of **3** is simply stacking of the $[CeB_5O_9]$ layers along the *b*-axis (Figure 6a). Again the borate framework is 2D, but the layers are interlinked by Ce−O bonds; thus, the structure is 3D with large cavities. The $[CeB_5O_9]$ layer can also be described by $[B_5O_{11}]$ as a FBB ($5\infty_2$:($3\Delta + 2T$)) as shown in Figure 6b. This is also a common borate unit found in other borates, such as nasinite ($Na_2[B_5O_8(OH)] \cdot 2H_2O$),[19] which contains a similar $Na[B_5O_9]$ layer, but additional Na ions are present between the layers so as to compensate for the negative charge.

The rare earth atoms are located around the center of the nine-membered borate rings and are further coordinated by the oxygen atoms on the borate side chains or water molecules in these structures. In the structure of $Nd[B_9O_{13}(OH)_4]H_2O$, the Nd atom is located at the center of the nine-membered ring with an average Nd−O distance of 2.519 Å to the six O atoms of the nine-membered ring. The total coordination number of Nd is 9 with three other oxygen atoms from the side chains with an average Nd−O distance of 2.454 Å. For $Pr[B_8O_{11}(OH)_5]$, the structure refinement clearly indicated a splitting of the Pr into two nearby positions with occupation of 0.93 (Pr1A) and 0.07 (Pr1B), respectively. The minority position Pr1B is located more closely to the center of the nine-membered ring with an average Pr−O distance of 2.532 Å, while the Pr1A position stays slightly away from the center with a longer average Pr−O distance (2.610 Å). The coordination polyhedron of the Pr1A position is 10-fold, of which six are the oxygen atoms from the nine-membered ring and four from the side chains. It is obvious that the larger rare earth cations tend to stay away from the center of the nine-membered ring largely due to the steric effect, and this is in fact in accordance with the observation that the larger rare earth cations prefer the octaborate **1** (from La to Nd) and smaller ones to the nonaborate **2** (from Pr to Eu). The radius of praseodymium cation happens to be about the critical value for these two structures; hence, it could be present in both structures. Furthermore, the splitting of the Pr position in the structure of $Pr[B_8O_{11}(OH)_5]$ can be considered as an indication of its intermediate situation. The steric effect of the rare earth cations is further evidenced in the structure of **3**. The cerium atoms in this hydrated pentaborate are well away from the center of the nine-membered ring as shown in Figure 6a with an average Ce−O distance of 2.615 Å. The coordination number of the Ce atom is ten, and again six of them are from the nine-membered ring and four respectively from the borate sheet, NO_3 group, and water molecules in the structure.

The hydroxyl groups in the structures of the hydrated polyborates cannot be precisely located in the structure refinements. The bond valence sums (BVS) calculations[20] show that the hydrogen atoms are bonded exclusively to the terminal oxygen atoms of the borate layers in $Pr[B_8O_{11}(OH)_5]$ and $Ce[B_5O_8(OH)]NO_3 \cdot 3H_2O$. For $Nd[B_9O_{13}(OH)_4] \cdot H_2O$, the terminal oxygen atoms on the borate framework are one short than the hydroxyl groups required to balance the charge. Bearing in mind that the structure of **2** is in fact a three-dimensional porous polyborate framework, the hydrogen atom may delocalize and give rise to a negatively charged borate framework. The BVS calculation, however, shows that this hydrogen atom is likely to be located near O1 in the borate side chain.

In a broad sense, compound **3** may also be considered as a microporous phase, if the ionic interaction (Ce−O bond) is taken into account in the frameworks. The cavity in the structure is one-dimensional along the *a*-axis. In fact, the cavity is quite large, accommodating one NO_3^- and three water molecules per formula. TGA measurements for $La[B_8O_{11}(OH)_5]$ (**1**), $Nd[B_9O_{13}(OH)_4] \cdot H_2O$ (**2**), and $Ce[B_5O_8(OH)]NO_3 \cdot 3H_2O$ (**3**) may well be interpreted based on the structure information. $La[B_8O_{11}(OH)_5]$ shows single-step weight loss (7.94 wt %) at about 300 °C, originating from the dehydration of the hydroxyl groups. The $Nd[B_9O_{13}(OH)_4] \cdot H_2O$ sample loses the weight in a stepwise manner upon heating. The first step (4.2 wt %) from 270 to 490 °C corresponds to the loss of the guest water molecules and partial dehydration of the framework, and the weight loss (6.3 wt %) between 500 and 660 °C may be related to the dehydra-

(19) Corazza, E.; Menchetti, S.; Sabelli, C. *Acta Crystallogr.* **1975**, *B31*, 2405.

(20) Brese, N. E.; O'Keeffe, M. *Acta Crystallogr.* **1991**, *B47*, 192.

tion and the collapse of the framework. The thermal behavior of $Nd[B_9O_{13}(OH)_4]\cdot H_2O$ is rather similar to that of microporous materials, which is consistent with the borate framework structure of **2**. The thermal behavior of **3** is rather similar to **2** but with several weight-loss steps. The first loss below 100 °C is related to the loss of guest water, while the second and third steps from 150 to 600 °C may be related to the decomposition of the nitrate and dehydration of the hydroxyl groups, respectively.

Crystal Structure of β-LaB_5O_9. The FBB in **5** is a $[B_5O_{12}]$ ($2T + 3\Delta$) unit as shown in Figure 7a, consisting of a three-ring ($2T + \Delta$) and two BO_3 (Δ) groups. The three-ring and a BO_3 group are linked, forming a nine-membered ring borate sheet (Figure 7b). This borate sheet is buckled approximately parallel to the $a-c$ plane of the structure. In addition, the nine-membered ring is rather distorted so that only five O atoms are effectively coordinated to the central La atom. Although the borate sheet in **5** is substantially different from that found in the hydrated polyborates, the presence of the nine-membered ring in this anhydrous polyborate provides concrete evidence that the nine-membered borate ring is favorable for the large cations. It is also worth mentioning that several other nine-membered window systems were identified recently in some lamellar or microporous germanates.[21−23] The structure principle of these systems is certainly different from borates; it does show that the nine-membered ring is a common structural geometry present in various systems. The 9-ring sheets are interlinked by additional BO_3 groups; thus, the β-LaB_5O_9 is a 3D framework structure as shown in Figure 7c, which contains 16-membered rings. The coordination polyhedron of lanthanum is 9-fold. β-LnB_5O_9 is formed only for La and Ce presumably because their larger cation size can stabilize the nine-membered ring fragment.

For the smaller lanthanides, the α-LnB_5O_9[9] structure is preferred. The FBB in the α-LnB_5O_9 structure is a $[B_5O_{11}]$ unit (also $2T + 3\Delta$) (Figure 7d) consisting of a double-three-ring ($2T + 2\Delta$) and a BO_3 group. The double-three-ring unit ($[B_4O_9]$) can be derived by condensation of O4 and O6 atoms of the $[B_4O_{10}]$ group in the β-LnB_5O_9 structure. The borate framework in the α-LnB_5O_9 structure is three-dimensional, formed by two interpenetrating borate subframeworks.[9] The rare earth atoms are located in a nine-coordination polyhedron. The thermal stability of β-LaB_5O_9 is higher than that of α-LnB_5O_9 and no thermal effect was observed up to 1000 °C. As previously reported, the α-LnB_5O_9 decomposed between 750 and 900 °C to the metaborates (Pr−Tb) or the orthoborates (Dy−Er).[9]

Photoluminescence. To exploit the possibility of using the β-LaB_5O_9 as a host of luminescent materials, a series of Eu-doped samples LaB_5O_9:$x$$Eu^{3+}$ were prepared. LaB_5O_9:Eu^{3+} exhibits efficient deep-red emission under UV excitation as shown in Figure 8a. The broad excitation band at about 200−310 nm (insert in Figure 8a) is the typical charge-transfer transition of $O \rightarrow Eu^{3+}$.

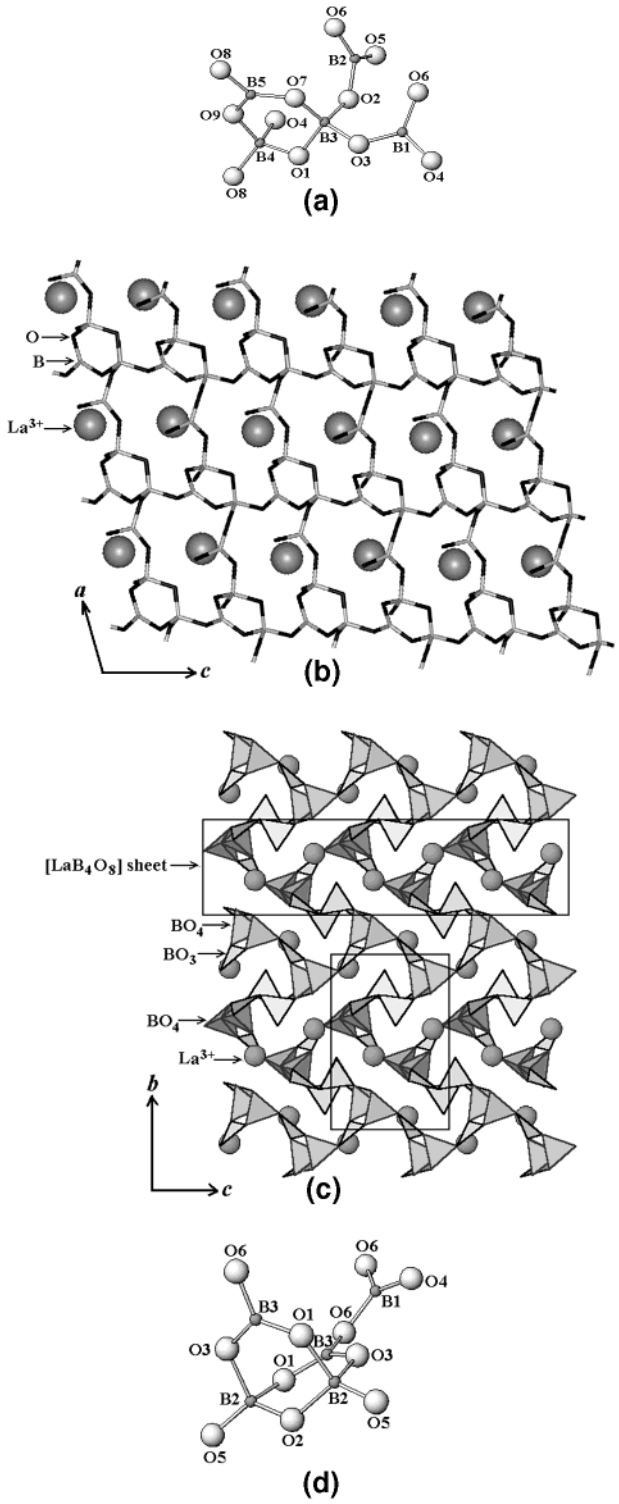

Figure 7. (a) Fundamental building block in the structure of β-LaB_5O_9. (b) $[LaB_4O_8]$ sheets containing nine-membered rings in the structure of β-LaB_5O_9. (c) Overview of the structure of β-LaB_5O_9 viewed along the (100) direction, in which the buckled $[LaB_4O_8]$ sheet is emphasized in a rectangle. (d) Fundamental building block in the structure of α-LnB_5O_9.

The emission lines ranging from 580 to 720 nm originate from the optical transitions from $^5D_0$ to ^7F_J ($J = 0-4$). The $^5D_0 \rightarrow {}^7F_0$ is a single emission line, indicating that only one crystallographic cation site is available in the host. Furthermore, the dominant electric dipole−dipole transition ($^5D_0 \rightarrow {}^7F_2$) implies that the europium cations occupy the non-centrosymmetric site. All these observa-

(21) Bu, X.; Feng, P.; Gier, T. E.; Zhao, D.; Stucky, G. D. *J. Am. Chem. Soc.* **1998**, *120*, 13389.
(22) Feng, P.; Bu, X.; Stucky, G. D. *Chem. Mater.* **1999**, *11*, 3025.
(23) Conradsson, T.; Zou, X.; Dadachov, M. S. *Inorg. Chem.* **2000**, *39*, 1716.

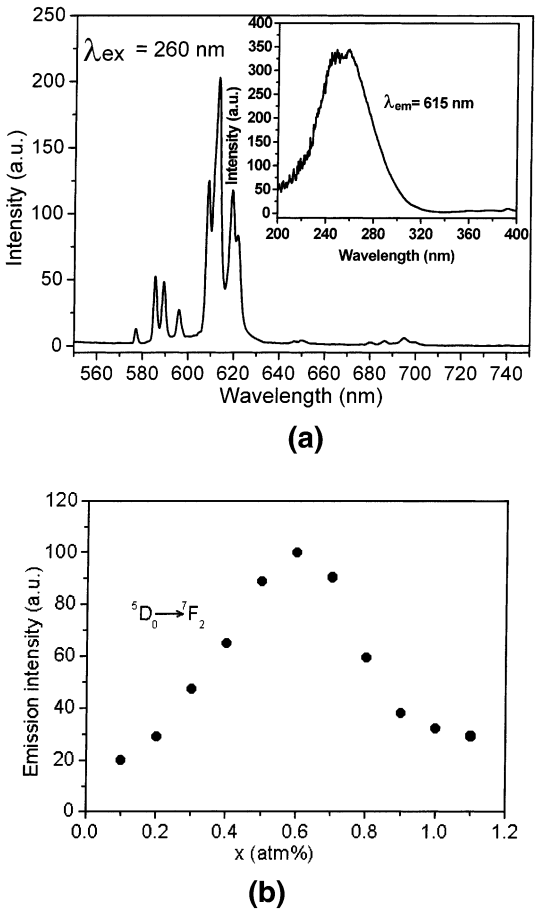

Figure 8. (a) Emission and excitation (insert) spectra of LaB_5O_9:Eu. (b) Variation of the emission intensity with the doping concentration in the LaB_5O_9:*x*Eu system.

tions are in good agreement with the structural studies. In addition, the luminescent intensity increases with the doping concentration up to $x = 0.6$ at.%, beyond which the luminescence declines very quickly (Figure 8b). The reason for this low quenching concentration may be related to the structural distortion induced by substitution of smaller cation Eu^{3+} for La^{3+} in the β-LaB_5O_9 structure. For the α-LnB_5O_9 system, EuB_5O_9 and GdB_5O_9 are isostructural; thus, one expects less structure distortion for the EuB_5O_9−GdB_5O_9 system. The luminescent study did show that the quenching concentration is significantly higher for GdB_5O_9:Eu. In this system, the luminescence intensity increases as the doping concentration increases up to $x = 10$ at. % and then it remains almost constant beyond this doping level.[9]

In conclusion, we have further demonstrated molten boric acid is a promising reaction medium for synthesizing hydrated rare earth polyborates. Diverse hydrated polyborates, from pentaborate to nonaborates, were obtained with this method. The structures of these hydrated polyborates are quite interesting and can be related to a hypothetical graphite-like borate sheet by removing the B_3O unit in certain ways. These hydrated polyborates can be used as precursors to synthesize anhydrous rare earth polyborates at moderate temperature. The obtained anhydrous pentaborates have two polymorphs, α-LnB_5O_9 and β-LnB_5O_9, depending on the rare earth cation size. These phases are new rare earth polyborates that are metastable at high temperature and, therefore, can only be synthesized by this low-temperature procedure. This is also the reason that these phases were not observed in the Ln_2O_3−B_2O_3 phase diagram. In addition, the europium-doped β-LaB_5O_9, as well as that of α-GdB_5O_9 reported previously, show promising deep-red emission. But using these rare earth polyborates as the hosts of luminescent materials will need further modification and optimization of the preparation process.

Acknowledgment. We are thankful for the financial support from NSFC and State Key Basic Research Program of China.

Supporting Information Available: Crystallographic information files (CIF) for $Pr[B_8O_{11}(OH)_5]$, $Nd[B_9O_{13}(OH)_4]\cdot H_2O$, $Ce[B_5O_8(OH)]NO_3\cdot 3H_2O$, and LaB_5O_9, as well as the bond lengths and angles for LaB_5O_9 (PDF). This material is available free of charge via the Internet at http://pubs.acs.org.

CM030004D